Paleoclassical H-Mode Pedestal Modeling*

J.D. Callen, University of Wisconsin, Madison, WI 53706-1609
T.H. Osborne, R.J. Groebner, H.E. St. John, General Atomics, San Diego, CA, 92186-5608
A.Y. Pankin, G. Bateman, A.H. Kritz, K. McFarland, Lehigh Univ., Bethleham, PA 18015-3182
W.M. Stacey, Georgia Tech, Atlanta, GA 30332

At the recent IAEA Chengdu meeting, the paleoclassical model of radial electron heat transport was compared with experimental results from a number of toroidal plasma experiments, including H-mode edge pedestals. This presentation will: 1) review comparisons of the paleoclassical model with H-mode pedestal data from DIII-D, 2) present some additional recent comparisons, and 3) highlight areas where additional work is needed. Specific comparisons to be presented include:

1) Ratio of the electron temperature to density gradient between the pedestal symmetry point and separatrix for which the paleoclassical prediction is $\eta_e \equiv L_{n_e}/L_{T_e} \simeq 2$.

2) Comparison of the paleoclassical radial electron heat diffusivity $\chi_e^{\rm pc}$ to the transport analysis χ_e, which both scale roughly as $T_e^{-3/2}$ near the separatrix.

3) Predictive transport analysis of the edge T_e profile in the pedestal region using the ASTRA code with $\chi_e^{\rm pc}$ dominating for $\rho \gtrsim 0.9$.

4) Pedestal height prediction determined from balancing the collisional (Alcator-scaling) paleoclassical $\chi_e^{\rm pc}$ against gyroBohm scale transport: $\beta_e^{\rm ped} \equiv n_e^{\rm ped} T_e^{\rm ped}/(B^2/2\mu_0) \simeq (0.032/f_\# A_i^{1/2})(\bar{a}/\bar{R}q)(\eta_\parallel^{\rm nc}/\eta_0)$, in which $f_\# \sim 1$ is a gyroBohm multiplier for T_e transport.

Extensions of the paleoclassical transport model to particle and ion heat transport will also be discussed. Finally, some additional theory, modeling and experimental tests needed for further testing and validation of the paleoclassical model will be discussed.

*Research supported by U.S. DoE grants and contracts DE-FG02-92ER54139 (UW-Madison), DE-FC02-04ER54698 (GA), DE-FG02-92ER54141 (Lehigh), and DE-FG02-00ER54538 (GaTech).

PALEOCLASSICAL H-MODE PEDESTAL MODELING

J.D. Callen, University of Wisconsin, Madison, WI 53706-1609
T.H. Osborne, R.J. Groebner, H.E. St. John, General Atomics, San Diego, CA 92186
A.Y. Pankin, G. Bateman, A.H. Kritz, K. McFarland, Lehigh U., Bethleham, PA 18015
W.M. Stacey, Georgia Tech, Atlanta, GA 30332

12th US-EU Transport Taskforce Workshop, April 17-20, 2007, San Diego, CA

- **Theses:**

  1) The paleoclassical model provides a lower limit (i.e., for no μturb.) on radial electron heat transport in an H-mode pedestal that approximately predicts the observed χ_e and T_e profiles in the DIII-D pedestal region.

  2) Electron pedestal height is set by the transition in dominant transport mechanism from paleoclassical in edge to ITG/DTEM microturbulence in hot core $\Longrightarrow$ $\beta_e^{\rm ped} \simeq 0.032\,[\bar{a}/(\bar{R}q f_{\#} A_i^{1/2})](\eta_{\|}^{\rm nc}/\eta_0)$.

- **Outline:**

  Assumptions used in paleoclassical T_e pedestal model
  Regions, paleoclassical regimes in DIII-D H-mode edge pedestal
  Paleoclassical model and DIII-D tests for edge χ_e, T_e profiles and $\beta_e^{\rm ped}$
  Extensions of paleoclassical model
  Summary and issues for future

Paleoclassical Model For H-Mode T_e Edge Pedestal

- **Model addresses H-mode T_e pedestals between ELMs for which:**

  Fluctuations levels are usually reduced (relative to L-modes).

  Anomalous transport due to drift-wave-type microturbulence, which is usually scaled to $D^{\rm gB} \sim (\varrho_S/a)(T_e/eB) \propto T_e^{3/2}/aB^2$ may be smaller than $\chi_e^{\rm pc} \sim \#\,\eta/\mu_0 \propto a^{1/2}T_e^{-3/2}$

  $\Longrightarrow$ for $T_e \lesssim T_e^{\rm crit} \simeq B({\rm T})^{2/3}a({\rm m})^{1/2}$ keV ~ 1 keV paleoclassical T_e transport dominates?

- **Key assumptions for paleoclassical model of H-mode T_e pedestal are:**

  1) In "near transport equilibrium" between Type I ELMs, electron heat transport is dominated by paleoclassical radial electron heat transport.

  2) T_e on divertor separatrix is fixed — by balancing heat flow across separatrix against parallel electron heat conduction on open field lines outside it.[1]

  3) The n_e profile in the pedestal is fixed — by balancing neutral fueling against radial particle diffusion,[2] **fitted by a tanh profile.**[1]

---

[1] G.D. Porter, J. Moller, M. Brown, C. Lasnier, and The DIII-D Team, Phys. Plasmas **5**, 1410 (1998).

[2] W. Engelhardt, W. Feneberg, J. Nucl. Mater. **76&77**, 518 (2978); F. Wagner and K. Lackner, *Physics of Plasma-Wall Interactions in Controlled Fusion*, NATO ASI Ser. B, Phys., V. 131, p. 931; M.A. Mahdavi *et al.*, Nucl. Fusion **42**, 52 (2002); R.J. Groebner *et al.*, Nucl. Fusion **44**, 204 (2004).

Paleo Model: ***Paleoclassical Radial Electron Heat Transport***

- **Physical process:**[3] **electron guiding centers diffuse radially with thin annuli of poloidal magnetic flux, carrying electron heat with them.**

- **Paleoclassical radial electron heat transport operator $\langle \vec{\nabla}\cdot \vec{Q}_e^{\rm pc}\rangle$ is**

$$\boxed{\frac{\partial}{\partial V}\langle \vec{Q}_e^{\rm pc}\cdot\vec{\nabla}V\rangle = -\frac{M+1}{V'}\frac{\partial^2}{\partial\rho^2}\left(V'\bar{D}_\eta\,\frac{3}{2}n_eT_e\right), \quad M\simeq\frac{1}{\pi\bar{R}\,q(\rho)/\lambda_e+1/n_{\rm max}}\lesssim 10.}$$

- **The diffusive part indicates a paleoclassical electron heat diffusivity of**

$$\boxed{\chi_e^{\rm pc}\equiv\frac{3}{2}(M+1)D_\eta} \quad\Longrightarrow\quad \begin{cases} \chi_{eI}^{\rm pc}\simeq\dfrac{3}{2}\left(\dfrac{1}{\pi\bar{\delta}_e|q'|}\right)^{1/2}\dfrac{\eta_\parallel^{\rm nc}}{\mu_0}, & \text{collisionless } (M\sim 10)\\ & \lambda_e>\ell_{\rm max}\equiv\pi\bar{R}q\,n_{\rm max},\\ \chi_{eII}^{\rm pc}\simeq\dfrac{3}{2}\dfrac{\eta_\parallel^{\rm nc}}{\eta_0}\dfrac{v_{Te}}{\pi\bar{R}q}\dfrac{c^2}{\omega_p^2}, & \text{collisional } (10\gtrsim M>1)\\ & \ell_{\rm max}>\lambda_e>\pi\bar{R}q\ ,\\ \chi_{eIII}^{\rm pc}\simeq\dfrac{10^3\,Z_{\rm eff}}{T_e({\rm eV})^{3/2}}, & \text{near separatrix } (M<1)\\ & \pi\bar{R}q>\lambda_e>\pi R\ , \end{cases}$$

where $D_\eta\equiv\eta_\parallel^{\rm nc}/\mu_0$ is the magnetic diffusivity, $\eta_\parallel^{\rm nc}$ is the parallel neoclassical resistivity, $\lambda_e\equiv v_{Te}/\nu_e$ is the collision length and $\ell_{\rm max}=\pi\bar{R}q\,n_{\rm max}$ is diffusing field line length with $n_{\rm max}\equiv(\pi\bar{\delta}_e|q'|)^{-1/2}$ in which $\bar{\delta}_e\equiv c/\omega_p\bar{a}$ is a normalized electromagnetic skin depth.

[3] J.D. Callen, "Derivation of paleoclasssical key hypothesis," Phys. Plasmas **14**, 040701 (2007) (Originally UW-CPTC 06-8R, January 2007).

Pedestal: ***H-Mode Edge Pedestals In DIII-D Will Be Described In Terms Of 3 Regions: I, II, III***

- **I: Core hot plasma, inside top of T_e pedestal, $\rho < \rho_{\rm ped} \equiv \rho_T - 2\Delta_T \simeq 0.935$, in collisional ($T_e \lesssim 1.1$ keV) and collisionless pc regimes.**

- **II: Top half of pedestal, top of T_e pedestal down to T_e symmetry point ρ_T, $0.935 < \rho < \rho_T \simeq 0.978$, in collisional pc regime.**

- **III: Bottom half of pedestal, $\rho_T < \rho < 1$ (separatrix), in near-separatrix pc regime, where $T_e(\rho)$ has + curvature.**

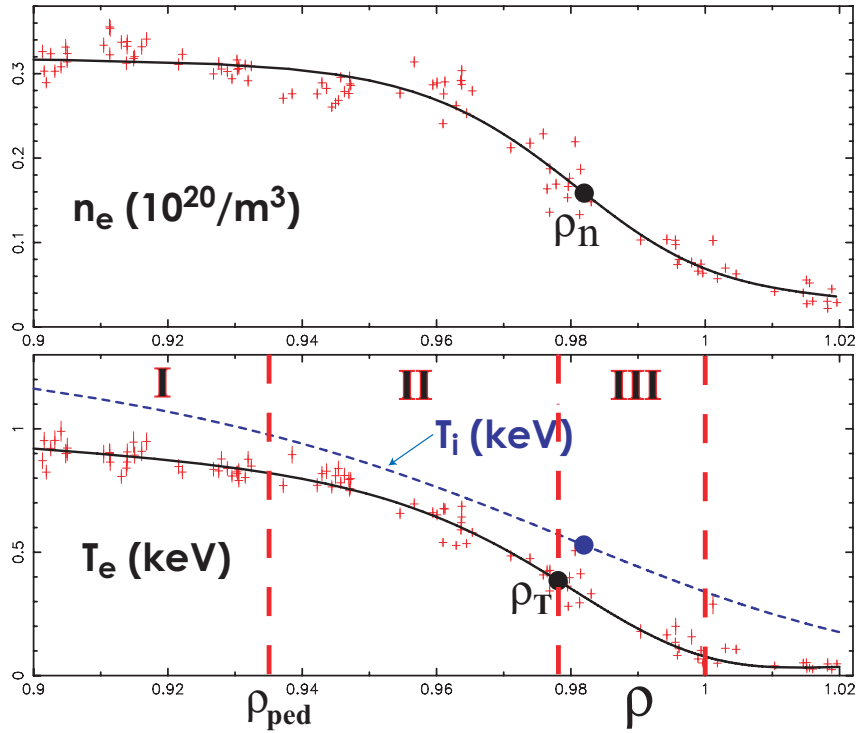

Figure 1: Edge pedestal n_e, T_e profiles for DIII-D shot 98889, averaged over 80-99% of time to next ELM crash, around 4500 ms. Lines show tanh fits to Thomson scattering data with symmetry points ρ_n, ρ_T.

Pedestal Heat Diffusivities: ***H-Mode Edge Pedestals In DIII-D Have Minimum In χ_e Near T_e Symmetry Point ($\rho_T \simeq 0.978$)***

- **χ_e varies significantly in the edge pedestal region ($\rho \gtrsim 0.9$).**
- **For $\rho \nearrow$, χ_e in pedestal region:**
  - **I: first decreases with ρ,**
  - **II: reaches a minimum at $\rho \sim 0.97$,**
  - **III: increases strongly for $\rho > 0.97$.**
- **χ_e at separatrix is rather large ($\sim$ 3 m^2/s), but it is small at its minimum in the pedestal ($\sim$ 0.55 m^2/s).**
- **Next two viewgraphs show interpretive and predictive modeling of $\chi_e(\rho)$, $T_e(\rho)$ with the paleoclassical $\chi_e^{\rm pc}(\rho)$.**

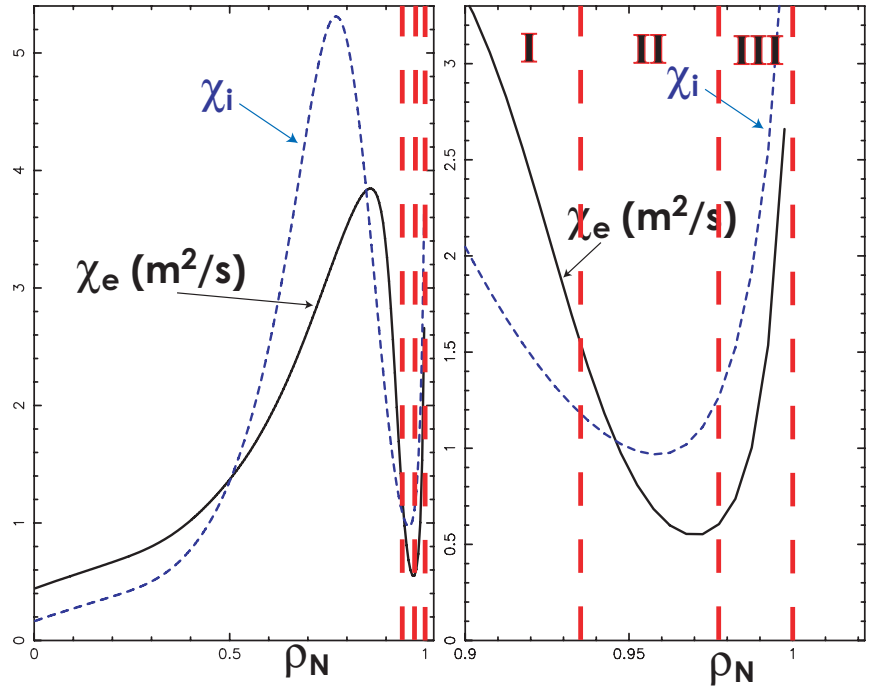

Figure 2: Electron, ion thermal diffusivities obtained from ONETWO transport analysis of DIII-D shot 98889, averaged over 80-99% of time to next ELM crash, at $\sim$ 4500 ms. An approximate cylindrical model of edge neutral effects has been used.

Paleoclassical χ_e^{pc} Agrees Well With Interpretive χ_e In II,III

- **Key assumption for interpretive modeling[a] is $(Q_e/Q)_{sep}$, which is the electron fraction of power flow through separatrix.**
- **χ_e^{pc} agrees very well with interpretive χ_e in region III and reasonably well in II.**
- **But min χ_e^{pc} can be too high by factor $\sim$ 2–10 in region II — discussed more at end of talk.**
- **Strong increase of χ_e with ρ in region III due to $\chi_{eIII}^{pc} \propto T_e^{-3/2}$.**
- **In regions II, III no other χ_e model works as well[a,b] as χ_e^{pc}.**

[a] W.M. Stacey and R.J. Groebner, Phys. Plasmas **13**, 072510 (2006); *ibid,* **14**, 012501 (2007)

[b] W.M. Stacey and T.E. Evans, PoP **13**, 112506 (2006).

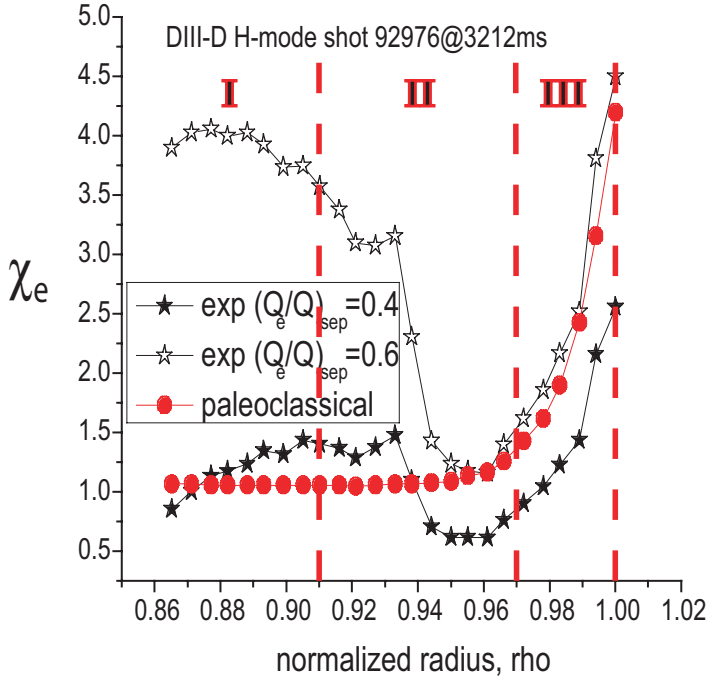

Figure 3: Interpretive [W.M. Stacey and R.J. Groebner, PoP **13**, 072510 (2006)] profiles of χ_e and χ_e^{pc} (in m^2/s) in pedestal similar to Fig. 1. $(Q_e/Q)_{sep}$ is electron fraction of power flow through separatrix.

ASTRA Modeling of DIII-D Shot Like 98889 Illustrates Role Of Micro-Turbulence Versus Paleoclassical In Edge

- **ITG/TEM, ETG dominant for $\rho < 0.85$ — in core (I).**
- **$\vec{E}\times\vec{B}$ flow shear has been used to reduce edge transport due to μ-turbulence.**
- **Paleoclassical χ_e dominant for $\rho > 0.9$ — edge (II, III).**
- **$T_e(\rho)$ is modeled well by combo of ITG/TEM,ETG (I: core) & paleo (II,III).**
- **Increasing $\chi_e^{\rm pc}$ as one approaches separatrix causes neutral or + curvature of T_e for $\rho > \rho_T \simeq 0.978$ (III).**

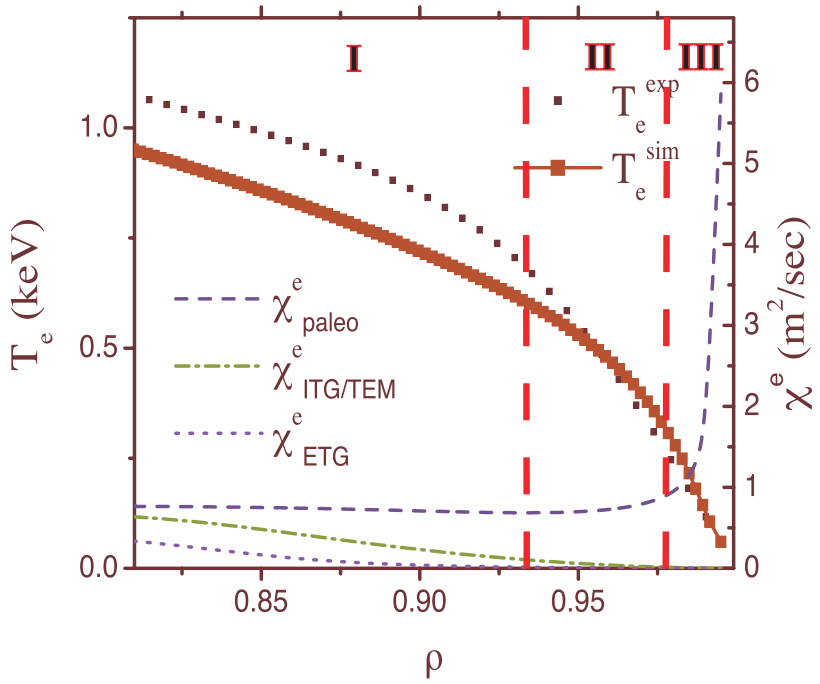

Figure 4: ASTRA modeling [Pankin et al., NF **46**, 403 (2006)] of DIII-D edge $T_e(\rho)$ in shot like 98889 in Fig. 1. Significant radial resolution is used, required — 500 radial points.

Brief Overview: ***Paleoclassical Model Of $T_e(\rho)$ In H-mode Edge***

- **Assume $n_e(\rho)$ profile is set by balancing neutral fueling, low D for stabilized RBMs in H-mode edge pedestal — Groebner, Mahdavi et al. model.[2]**

- **Assuming T_e profile is set by $\chi_{eIII}^{\rm pc}$ for $\rho > 0.978$ and collisional (Alcator scaling) $\chi_{eII}^{\rm pc}$ further inward yields paleoclassical predictions (p17 below):**

  $T_e \propto n_e^2$ and $\eta_e \equiv \partial \ln T_e/\partial \ln n_e \simeq 2$ near separatrix, for $\rho > \rho_T \simeq 0.978$ (region III),

  Maximum $|\vec{\nabla} T_e|$ near transition from region II to III at $\rho_T \simeq 0.978$,

  S-shaped T_e profile: $\partial^2 T_e/\partial\rho^2 > 0$ in region III, $\partial^2 T_e/\partial\rho^2 < 0$ in region II.

- **Pedestal electron pressure $p_e^{\rm ped} \equiv n_e^{\rm ped} T_e^{\rm ped}$ set by balancing Alcator-scaling collisional $\chi_{eII}^{\rm pc} \simeq \dfrac{3}{2}\dfrac{v_{Te}}{\pi \bar{R} q}\dfrac{c^2}{\omega_p^2}\dfrac{\eta_\parallel^{\rm nc}}{\eta_0} \propto \dfrac{T_e^{1/2}}{n_e q}$ against $\chi_e^{\rm gB} \simeq f_\# \, 3.2 \dfrac{T_e^{3/2} A_i^{1/2}}{\bar{a} B^2}$ is**

$$\boxed{\beta_e^{\rm ped} \equiv \frac{n_e^{\rm ped} T_e^{\rm ped}}{B^2/2\mu_0} \simeq 0.032 \frac{\bar{a}}{f_\# \bar{R} q A_i^{1/2}} \left(\frac{\eta_\parallel^{\rm nc}}{\eta_0}\right),}$$

near transition from I to II,

in which $\bar{a} \simeq [2\kappa^2/(1+\kappa^2)]^{1/2} a \sim a$, $\bar{R} \simeq R_0$ and $f_\#$ is "gyroBohm T_e transport factor," which has a threshold-type behavior and depends on T_e/T_i, magnetic shear, ν_{*e} etc.

Tests Of $T_e \propto n_e^2$ Paleoclassical Prediction Near Separatrix

- AUG[a] first found $T_e \propto n_e^2$ and $\eta_e \simeq 2$ near separatrix.
- Paleoclassical prediction of $T_e \propto n_e^2$ is tested against the DIII-D pedestal database by

  1) using for reference values the T_e, n_e at the ρ where the tanh fit T_e is 0.1 keV ($\sim$ separatrix),

  2) determining T_e, n_e values at the T_e symmetry point ρ_T, and

  3) plotting the ratio of T_e at the symmetry point to its reference value versus the square of the corresponding density ratio.
- Results are consistent with the paleoclassical prediction for $T_e \lesssim 0.2$ keV, and bounded by it for higher T_e.

[a] J. Neuhauser *et al.* PPCF 44, 855 (2002) — see Fig. 5.

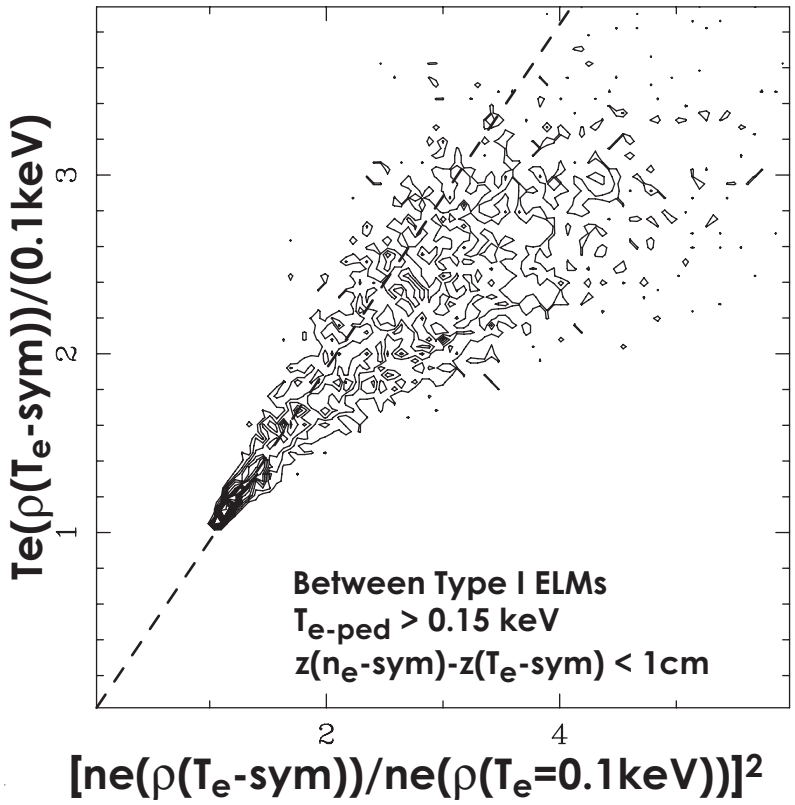

Figure 5: Probability contours from DIII-D database (9104 points) of T_e versus n_e^2 at symmetry point for T_e and n_e referenced to their values at the point where T_e is 0.1 keV. Dashed line indicates $T_e \propto n_e^2$ and hence $\eta_e = 2$.

Paleoclassical Model Predicts Pedestal Height $\beta_e^{\rm ped}$ In DIII-D

- **Pedestal T_e predicted by balancing collisional $\chi_{eII}^{\rm pc}$ against $\chi_e^{\rm gB}$ (viewgraph p9) yields $\beta_e^{\rm ped} \equiv n_e^{\rm ped} T_e^{\rm ped}/(B^2/2\mu_0) \simeq (0.032/f_\# A_i^{1/2})(\bar{a}/\bar{R}q)(\eta_\parallel^{\rm nc}/\eta_0)$.**

- **For a DIII-D deuterium case with $(\bar{a}/\bar{R}q)(\eta_\parallel^{\rm nc}/\eta_0) \simeq 0.08$, $\beta_e^{\rm ped} \simeq 0.18\%/f_\#$, which agrees with fit to data for $f_\# \simeq 0.82$.**

- **Paleoclassical magnitude and scaling are consistent with DIII-D pedestal database if $f_\# \simeq 0.6$–2 — range covers the large spread in data.**

- **Scaling needs to be tested in other tokamak experiments.**

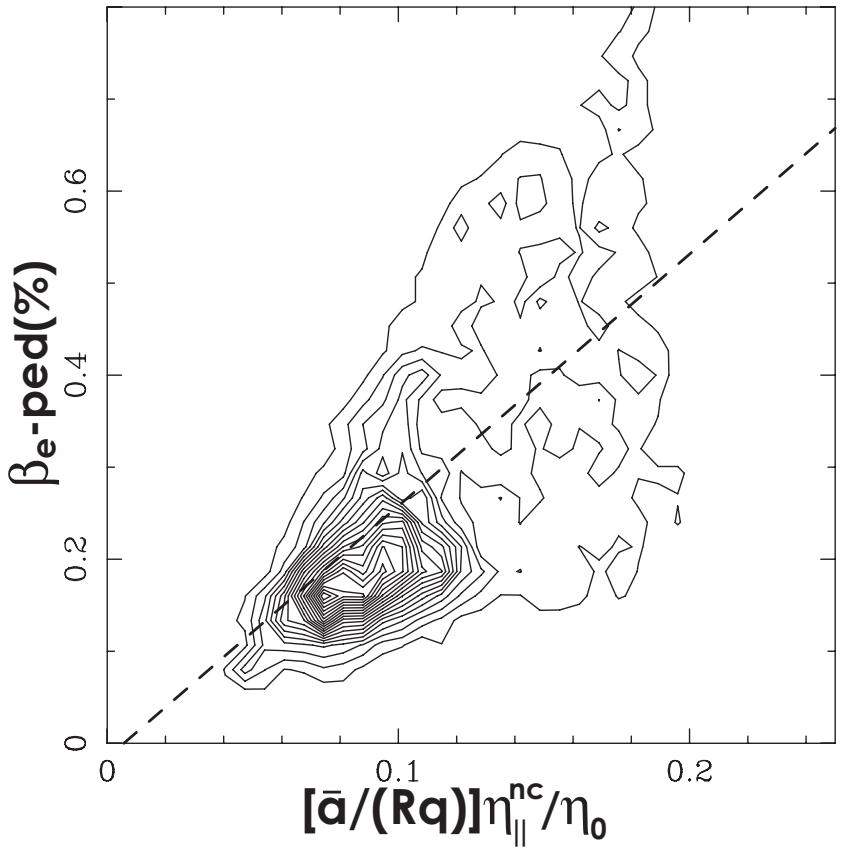

Figure 6: Probability contours from DIII-D database (9104 points) show $\beta_e^{\rm ped}$ varies roughly linearly (dashed line is a linear fit to data) with the paleoclassical model variable and has a bounded slope.

Other Implications, Extensions Of Paleoclassical Model

- **The form of the paleoclassical electron heat transport operator is different:**

  $\langle \vec{\nabla}\cdot\vec{Q}_e^{\rm pc}\rangle = -\frac{M+1}{V'}\frac{\partial^2}{\partial\rho^2}\left(V'\frac{3}{2}\bar{D}_\eta n_e T_e\right)$ **in contrast to usually assumed** $\frac{1}{V'}\frac{\partial}{\partial\rho}\left(V' n_e \chi_e \frac{\partial T_e}{\partial\rho}\right)$.

- **This different transport operator form has three important consequences:**

  A "heat pinch" type term $\propto T_e(\partial/\partial\rho)(V'\bar{D}_\eta n_e)$ **occurs naturally.**

  The "power balance" χ_e **is different from** $\chi_e^{\rm pc}$**:** $\chi_{e\rm PB}^{\rm pc} \simeq \dfrac{-\int_0^\rho d\rho\,(M+1)\frac{\partial^2}{\partial\rho^2}\left(V'\frac{D_\eta}{\bar{a}^2}\frac{3}{2}n_e T_e\right)}{n_e V'(1/\bar{a}^2)(-dT_e/d\rho)}$.

  To treat properly, the numerical algorithms in modeling codes may have to be modified.

- **Complete model of all paleoclassical transport processes is needed:**

  Present guess: density $D^{\rm pc} \simeq D_\eta$**, ion heat** $\chi_i^{\rm pc} \simeq (3/2)D_\eta$ **and toroidal mom.** $\chi_\zeta^{\rm pc} \simeq D_\eta$**, with natural pinch effects in all — similar to experimental results**[a,4] **in region III.**

  Also, an ambipolar potential and $E_r^{\rm pc}$ **likely in region II** $\Longrightarrow V_\zeta$ **edge boundary condition?**

- **Need to determine 2D structure of paleo transport in vicinity of separatrix:**

  A local field line (not flux surface) paleoclassical formalism is needed in region III, "on" and outside the divertor separatrix.

  Toroidal-current-induced poloidal flux (ψ_J) **needs to be distinguished from "vacuum" flux** (ψ_V) **produced by external shaping coils:** $\chi_e \sim \chi_{eIII}^{\rm pc}[\psi_J'/(\psi_J'+\psi_V')]$?

[4] D.R. Baker, R. Maingi, L.W. Owen, G.D. Porter, G.L. Jackson, J. Nuc. Mat. **241-243**, 602 (1997); L.D. Horton *et al.*, Nuc. Fus. **45**, 856 (2005).

SUMMARY

- **Paleoclassical model predictions for the H-mode pedestal in reasonable agreement[5] with DIII-D pedestal data are:**

  1) $\chi_e^{\rm pc}$ versus interpretive χ_e and predictively modeled T_e profile versus experimental T_e profile in regions III and (less so) II,

  2) positive or neutral T_e profile curvature and $\eta_e \simeq 2$ in region III, and

  3) $\beta_e^{\rm ped}$ prediction due to change from collisional paleoclassical ($\chi_{eII}^{\rm pc}$) to gyroBohm-scaled microturbulence-induced anomalous transport near transition from region II to I.

- **More tests on DIII-D pedestals and similar tests on pedestals in other H-mode tokamak plasmas are needed to further validate (or invalidate?) the paleoclassical T_e pedestal model.**

[5] J.D. Callen, T.H. Osborne, R.J. Groebner, H.E. St. John, A.Y. Pankin, G. Bateman, A.H. Kritz, W.M. Stacey, "Paleoclassical model for edge electron temperature pedestal," UW-CPTC 06-6, March 2007 (submitted to Phys. Rev. Lett.; available via `http://www.cae.wisc.edu/~callen`).

Issues Remaining To Validate Paleoclassical Pedestal Model

- **Further testing of the present paleoclassical T_e pedestal model:**

  When does paleoclassical model provide minimum T_e transport in H-mode pedestals?

  Is the transition from paleoclassical to ITG/TEM transport robust in determining $\beta_e^{\rm ped}$?

  Is predicted $\beta_e^{\rm ped}$ distinguishable from $\beta'_{\rm crit}\Delta$ ($\Delta \simeq 0.02a$) from peeling-ballooning modes?

- **Explore consequences of form of paleoclassical transport operator:**

  What are the magnitude and consequences of $\chi_{ePB}^{\rm pc}$ being less than $\chi_e^{\rm pc}$ in region **II**?

  Do numerical algorithms in modeling codes need to modified?

- **Other possible paleoclassical transport effects (yet to be derived):**

  Does density transport agree with paleoclassical model, including density pinch effect?

  Does ion heat transport in region **III** agree with paleoclassical prediction there?

  Are paleoclassical $E_r^{\rm pc}$ and toroidal flow transport important in pedestals?

- **2D transport effects in vicinity of divertor separatrix (yet to be derived):**

  What are effects of "poloidal" variation and mix of current, vaccuum poloidal fluxes?

  Comparisons with UEDGE modeling[1,6] of edge pedestals that obtain effective diffusivities that increase with ρ in region **III** via combination of $\|$, $\perp$ transport near separatrix.

[6] T.D. Rognlien, Plasma Phys. Control. Fusion **47**, A283 (2005).

Interpretive Modeling Sometimes Finds χ_{eII}^{pc} Way Too Large

- **In interpretive modeling of DIII-D shot 98889, Stacey finds much smaller χ_e in region II.**
- **Then, χ_e^{pc} is a factor ~ 10 larger than χ_e in II and (less so) III.**
- **But here, minimum interpretive χ_e is a factor ~ 5 smaller than interpretive ONETWO (p6) and predictive ASTRA (p8) inferences for the same shot.**
- **Discrepancy may be due to differences in how magnetic geometry near the separatrix is treated — should be resolved.**
- **Nonetheless, paleo model still gives "least unlikely" fit to data.**

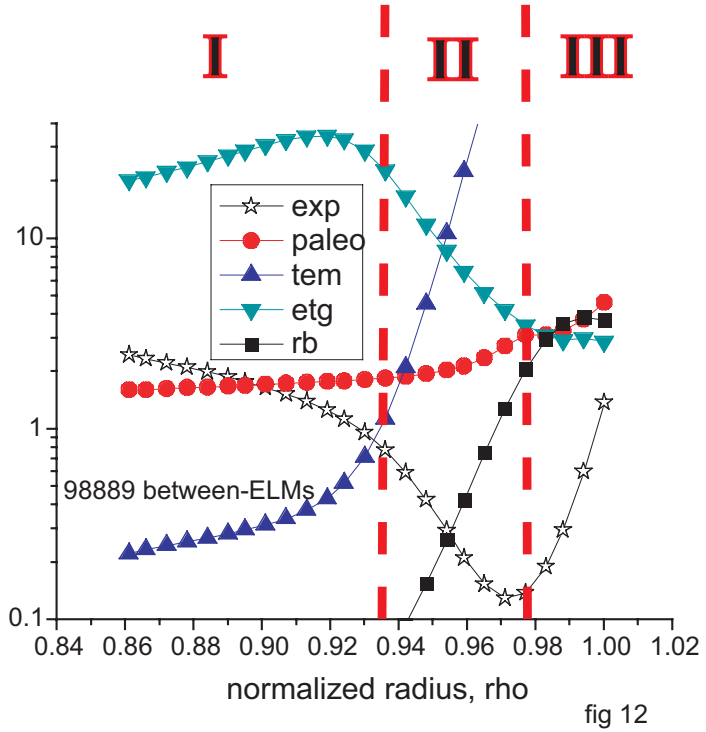

Figure 7: Interpretive [W.M. Stacey and R.J. Groebner, PoP **13**, 072510 (2006)] profiles of edge χ_e and χ_e^{pc} (in m^2/s) for shot 98889, as shown in Fig. 1. $(Q_e/Q)_{sep} = (Q_i/Q)_{sep} = 0.5$ has been assumed.

Annotated Bibliography

- Paleoclassical T_e H-mode pedestal model discussed in this presentation:

  J.D. Callen, T.H. Osborne, R.J. Groebner, H.E. St. John, A.Y. Pankin, G. Bateman, A.H. Kritz, W.M. Stacey, "Paleoclassical model for edge electron temperature pedestal," UW-CPTC 06-6, March 2007 (submitted to Phys. Rev. Lett.).

- Derivation of key hypothesis of the paleoclassical model:

  J.D. Callen, "Derivation of paleoclassical key hypothesis," Phys. Plasmas 14, 040701 (2007) (Originally UW-CPTC 06-8R, January 2007).

- More comprehensive comparisons of paleoclassical model to experimental data in 7 toroidal experiments, including H-mode T_e pedestal, and original papers on paleoclassical radial electron heat transport model:

  J.D. Callen, J.K. Anderson, T.C. Arlen, G. Bateman, R.V. Budny, T. Fujita, C.M. Greenfield, M. Greenwald, R.J. Groebner, D.N. Hill, G.M.D. Hogeweij, S.M. Kaye, A.H. Kritz, E.A. Lazarus, A.C. Leonard, M.A. Mahdavi, H.S. McLean, T.H. Osborne, A.Y. Pankin, C.C. Petty, J.S. Sarff, H.E. St. John, W.M. Stacey, D. Stutman, E.J. Synakowski, K. Tritz, "Experimental Tests Of Paleoclassical Transport," paper EX/P3-2, 21st IAEA Fusion Energy Conf., Chengdu, China, 16-21 October 2006 (submitted to NF).

  J.D. Callen, "Most Electron Heat Transport Is Not Anomalous; It Is a Paleoclassical Process in Toroidal Plasmas," Phys. Rev. Lett. 94, 055002 (2005).

  J.D. Callen, "Paleoclassical transport in low collisionality toroidal plasmas," Phys. Plas. 12, 092512 (2005).

  J.D. Callen, "Paleoclassical electron heat transport," Nucl. Fusion 45, 1120 (2005) (expanded version of 2004 IAEA Vilamoura paper TH/1-1).

- Preprints and reprints of these papers and reports are available from

  `http://homepages.cae.wisc.edu/~callen` and `http://www.cptc.wisc.edu`

Supplement: ***Simplified Transport Analysis Near Separatrix***

- **Assuming the dominant loss is due to the radial electron heat flux $\vec{q}_e$, the equilibrium electron energy balance equation is simply**

$$\frac{\partial}{\partial V}\langle \vec{q}_e \cdot \vec{\nabla} V \rangle = Q_e, \text{ net electron heating (collisional, joule + auxiliary − radiation).}$$

- **Integrating this over volume in region III from ρ to 1 (separatrix) yields $\langle \vec{q}_e \cdot \vec{\nabla} V \rangle_\rho \simeq \langle \vec{q}_e \cdot \vec{\nabla} V \rangle_1$ for a thin $(1 - \rho << 1)$ and weakly heated edge.**

- **Assuming the paleoclassical electron heat flux dominates, this result can be integrated inward from the separatrix at $\rho = 1$ to obtain $T_e(\rho)$ — assuming $n_e(\rho)$ is given (e.g., by Groebner-Mahdavi electron density profile model[2]):**

$$[V'(\chi_e^{\rm pc}/\bar{a}^2) n_e T_e]_\rho = [V'(\chi_e^{\rm pc}/\bar{a}^2) n_e T_e]_1 + \mathcal{O}[(1-\rho)^2].$$

- **Very near the separatrix where $n_e T_e \chi_{eIII}^{\rm pc} \sim n_e / T_e^{1/2}$, this result yields**

$$T_e(\rho) \simeq \left[\frac{n_e(\rho)\ [V'/\bar{a}^2]_\rho \quad Z_{\rm eff}(\rho)}{n_e(1)\ [V'/\bar{a}^2]_{\rho=1}\ Z_{\rm eff}(1)}\right]^2 T_e(1) \simeq \left[\frac{n_e(\rho)}{n_e(1)}\right]^2 T_e(1) \quad \Longrightarrow \quad T_e \propto n_e^2,\ \eta_e \simeq 2.$$